CHEMISTRY
A EUROPEAN JOURNAL

ChemPubSoc
Europe

DOI: 10.1002/chem.201302598

Preorganized Anion Traps for Exploiting Anion–π Interactions: An Experimental and Computational Study

Anne Bretschneider,[a] Diego M. Andrada,[b] Sebastian Dechert,[a] Steffen Meyer,[a] Ricardo A. Mata,*[b] and Franc Meyer*[a]

Abstract: 1,3-Bis(pentafluorophenylimino)isoindoline (A^F) and 3,6-di-*tert*-butyl-1,8-bis(pentafluorophenyl)-9*H*-carbazole (B^F) have been designed as preorganized anion receptors that exploit anion–π interactions, and their ability to bind chloride and bromide in various solvents has been evaluated. Both receptors A^F and B^F are neutral but provide a central NH hydrogen bond that directs the halide anion into a preorganized clamp of the two electron-deficient appended arenes. Crystal structures of host–guest complexes of A^F with DMSO, Cl^-, or Br^- (A^F:DMSO, A^F:Cl^-, and A^F_2:Br^-) reveal that in all cases the guest is located in the cleft between the perfluorinated flaps, but NMR spectroscopy shows a more complex situation in solution because of *E*,*Z*/*Z*,*Z* isomerism of the host. In the case of the more rigid receptor B^F, Job plots evidence 1:1 complex formation with Cl^- and Br^-, and association constants up to $960\,M^{-1}$ have been determined depending on the solvent. Crystal structures of B^F and B^F:DMSO visualize the distinct preorganization of the host for anion–π interactions. The reference compounds 1,3-bis(2-pyrimidylimino)isoindoline (A^N) and 3,6-di-*tert*-butyl-1,8-diphenyl-9*H*-carbazole (B^H), which lack the perfluorinated flaps, do not show any indication of anion binding under the same conditions. A detailed computational analysis of the receptors A^F and B^F and their host–guest complexes with Cl^- or Br^- was carried out to quantify the interactions in play. Local correlation methods were applied, allowing for a decomposition of the ring–anion interactions. The latter were found to contribute significantly to the stabilization of these complexes (about half of the total energy). Compounds A^F and B^F represent rare examples of neutral receptors that are well preorganized for exploiting anion–π interactions, and rare examples of receptors for which the individual contributions to the binding energy have been quantified.

Keywords: anion–π interactions · density functional calculations · hydrogen bonds · receptors · solution studies

Introduction

Anion–π interactions, that is, the attractive interactions between anions and electron-deficient π systems, have sparked significant interest in recent years.[1] Somewhat counterintuitive at first sight and thus controversially discussed for some time,[2] anion–π interactions are now considered as an important addition to the bouquet of established non-covalent interactions such as hydrogen bonds or CH–π and cation–π interactions, which form the basis of modern supramolecular chemistry.[3] After early reports on weak attractive interactions involving negatively charged residues and polarizable aryl groups in host–guest systems[4] a series of computational studies in 2002 supported the existence of attractive forces between electron-deficient arenes and anions centered above their π-cloud;[5] the term anion–π interaction was then coined.[5d] Shortly thereafter anion–π interactions were explicitly mentioned in crystallographic work for the first time, evidencing the location of chloride above a 1,3,5-triazine ring just as predicted by theory.[6] This marked the beginning of systematic experimental studies towards the detection, description, and targeted use of anion–π interactions in the solid state and in solution, mostly focusing on N-heterocycles such as 1,3,5-triazine or suitably substituted arenes such as pentafluorophenyl groups.[7] Anion–π interactions are now beneficially exploited in fields such as anion sensing,[8] anion transport through membranes,[9] or supramolecular assembly,[10] and they are even considered relevant for anion transport in biological systems.[11]

The number of reports that evidence anion–π interactions in the solid state is indeed increasing rapidly. However, experimental data that support and quantify the attractive interaction between anions and electron-deficient neutral arenes in the solution phase are still rather limited.[12] According to most estimates the free energy of binding

[a] A. Bretschneider, Dr. S. Dechert, S. Meyer, Prof. Dr. F. Meyer
Institut für Anorganische Chemie
Georg-August-Universität Göttingen
Tammannstrasse 4, 37077 Göttingen (Germany)
Fax: (+49) 551-3933063
E-mail: franc.meyer@chemie.uni-goettingen.de

[b] Dr. D. M. Andrada, Prof. Dr. R. A. Mata
Institut für Physikalische Chemie
Georg-August-Universität Göttingen
Tammannstrasse 6, 37077 Göttingen (Germany)
E-mail: rmata@gwdg.de

Supporting information for this article is available on the WWW under http://dx.doi.org/10.1002/chem.201302598.

($-\Delta G^0$) of anion–π interactions, which mainly results from electrostatic and anion-induced polarization contributions,[13] is likely rather low. A recent account concluded that the free energy of binding between halide anions and substituted phenyl groups is usually less than 1 kcal mol^{-1} in organic solvents,[12c] though the interaction may be energetically much more favorable in solvents with a large dielectric constant.[12b] In fact, most of the reported synthetic receptors combine anion–π interactions with other forces such as hydrogen bonding or salt bridges, and the anion–π interaction serves to augment anion binding in solution.[14] Thus, the extraction of thermodynamic data for the individual anion–π contribution to the interaction is complicated.[15]

Cooperativity of anion–π and other interactions such as hydrogen bonding may bring about reasonable binding constants for the hosting of anions by neutral receptors in solution, a situation that is still rather rare for systems that solely exploit anion–π contacts. Following this approach, just recently constants for chloride binding in the order of $3\times10^3\,M^{-1}$ in CD_3CN solution as well as the first crystallographic example of an anion–π interaction between an uncharged pentafluorophenyl derivative and a halide anion have been communicated.[15] However, most reported receptors that use directing hydrogen-bonding groups or charge assistance for anion–π interactions are conformationally quite flexible. This leads to positional diversity of the anion above the arene ring,[16] to competing intra- and intermolecular interactions[17] as well as to facile superseding of the anion–π contact by, for example, CH–anion hydrogen bonding or interactions between anion and solvent. Herein, we report two new neutral halide receptors A^F and B^F that trigger, through a directing N−H hydrogen bond, the binding of the anion into a preorganized clamp of two electron-deficient arenes exhibiting anion–π interactions. The design of these receptors is reminiscent of two mussel shell valves with the NH drawing the prey anion into the chamber.

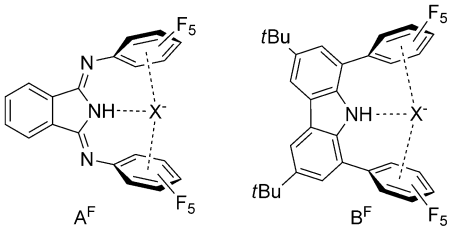

Whereas B^F is a particularly rigid system that enforces anion–π interactions once the anion is drawn into the open pocket between the pentafluorophenyl flaps, receptor A^F offers more conformational and configurational flexibility. The study of the anion binding with A^F and B^F employing both experimental and computational methods synergistically provides significant new information on the relevance of anion–π interactions and renders guidelines for the development of future new types of selective anion receptors that exploit such anion–π attractive contacts. Comparison is also established with their non-fluorinated derivates A^N and B^H (see below).

Results and Discussion

Synthesis and structural characterization of the receptors: Because of the highly electron-withdrawing nature of the pentafluorophenyl groups, established procedures for the synthesis of 1,3-bis(arylimino)isoindolines and 1,8-bis(aryl)-9*H*-carbazoles had to be modified in order to obtain the target receptors. 1,3-Bis(pentafluorophenylimino)-isoindoline (A^F) and the related 1,3-bis(2-pyrimidylimino)-isoindoline (A^N) were prepared by heating phthalocyanid and the corresponding amines (pentafluoroaniline or 2-aminopyrimidine, respectively) in *n*BuOH to reflux, using $CaCl_2$ as a catalyst (Scheme 1).[18] Due to the electron-deficient arenes, both amines are highly deactivated and thus yields were relatively low even after reaction times of up to three weeks. Additionally working under exclusion of water is strongly recommended as this prevents hydrolysis, which further minimizes the yield.

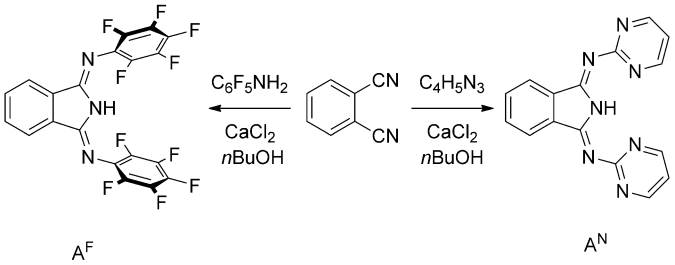

Scheme 1. Synthesis of receptors A^F and A^N.

The synthesis of 3,6-di-*tert*-butyl-1,8-bis(perfluorophenyl)-9*H*-carbazole (receptor B^F) and the non-fluorinated parent compound 3,6-di-*tert*-butyl-1,8-diphenyl-9*H*-carbazole (B^H) is depicted in Scheme 2. Following literature procedures Friedel–Crafts alkylation of the carbazole was performed, thus introducing *t*Bu groups into the backbone. Reaction of compound **1** with bromine then gave compound **2** in quantitative yield.[19] Because no suitable cross-coupling protocol was found to provide the target compounds directly from compound **2**, an additional step was included in which the bromo substituents were exchanged against boronic esters. This was achieved through in situ protection of the lithiated NH group with CO_2 followed by further addition of bis(pinacolato)diboron to give compound **3**. Finally, Suzuki–Miyaura cross-coupling conditions were applied to yield B^F and B^H in almost quantitative yields.[20]

X-ray diffraction analysis of single crystals of receptor B^F, obtained by reverse vapor diffusion of a solution of the receptor in chloroform into toluene, confirmed the molecular structure (Figure 1) and highlighted the preorganized anion binding site with the NH group "sting" directed into the space between the two pentafluorophenyl flaps, which are

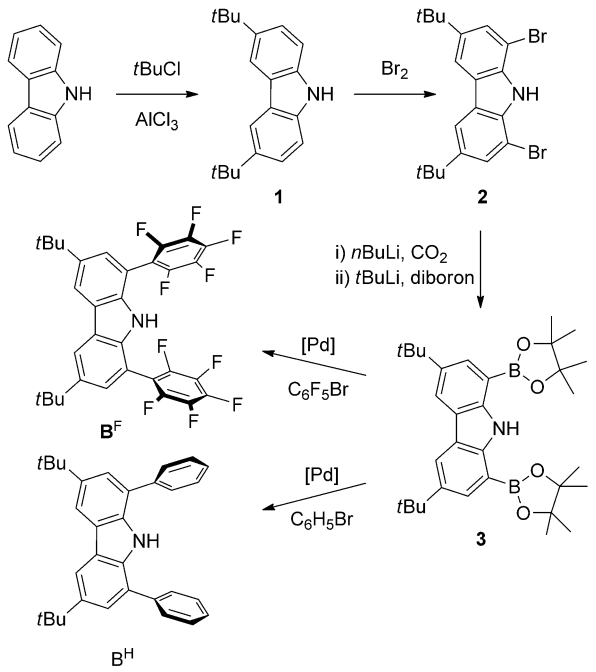

Scheme 2. Synthesis of receptors B^F and B^H.

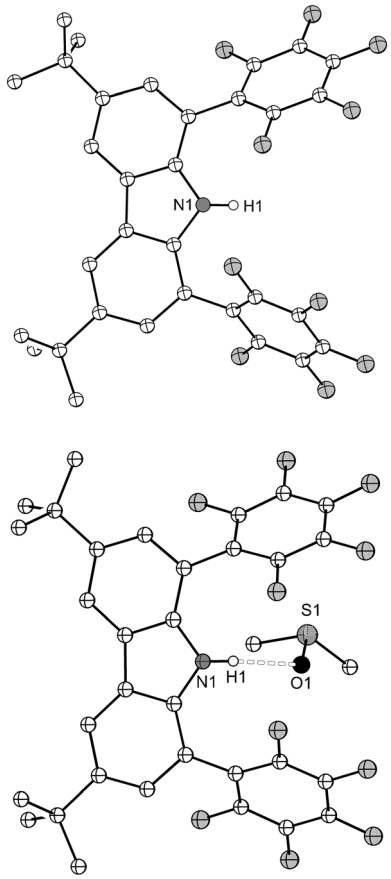

Figure 1. Molecular structure of receptor B^F (top) and the adduct B^F:DMSO (bottom). All hydrogen atoms except the NH proton are omitted for clarity.

severely tilted with respect to the carbazole backbone (angles between the C_6F_5 and the carbazole planes: 64/41°). A first indication for the ability of both receptors to bind guests within their chambers flanked by the pentafluorophenyl flaps was given by crystal structure analyses of their adducts with DMSO, namely B^F:DMSO (Figure 1 bottom) and A^F:DMSO (Figure 2), both obtained by slow evaporation of solutions of the compounds in DMSO. Most important, in B^F:DMSO the orientation of the pentafluorophenyl rings with respect to the carbazole backbone is barely changed (angles: 54/54°) compared to the free receptor, reflecting favorable preorganization. This suggests that any energetic penalty for adapting the shape of the receptor upon guest inclusion is low if the guest has the proper size, and hence it may suggest some favorable size selectivity.

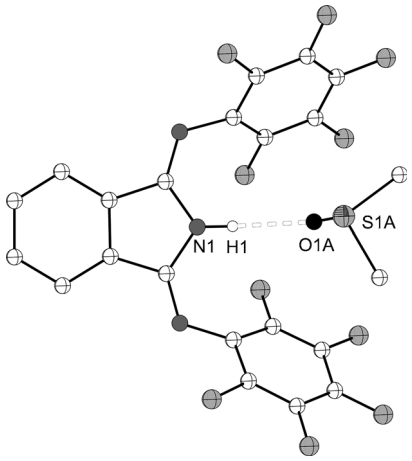

Figure 2. Molecular structure of the A^F:DMSO adduct. All hydrogen atoms except the NH proton are omitted for clarity.

Determination of the anion binding capabilities: The ability of the new receptors to bind anions was evaluated by determining, through NMR spectroscopy, the association constants (K_a) of the receptor with different halides. To obtain K_a values, ^1H and ^{19}F NMR titration experiments with $(Bu_4N)Cl$ and $(Bu_4N)Br$ as anion sources were carried out in different deuterated solvents. The stoichiometry of the host–guest complexes in solution was determined by Job's method.[21]

Type-A receptors: Preliminary studies with receptor A^F clearly demonstrated its ability to interact with halide anions, reflected by significant chemical shift changes upon addition of, for example, $(Bu_4N)Br$ (Figure 3). However, when looking at the system in more detail, problems arose to determine the stoichiometry as well as the stability constant. The ^1H and ^{19}F NMR spectra of A^F show the presence of two isomers (*Z*,*Z* or *E*,*Z*) in solution in a ratio of roughly 1:1, with only slight dependency on the solvent used or the temperature (Scheme 3).

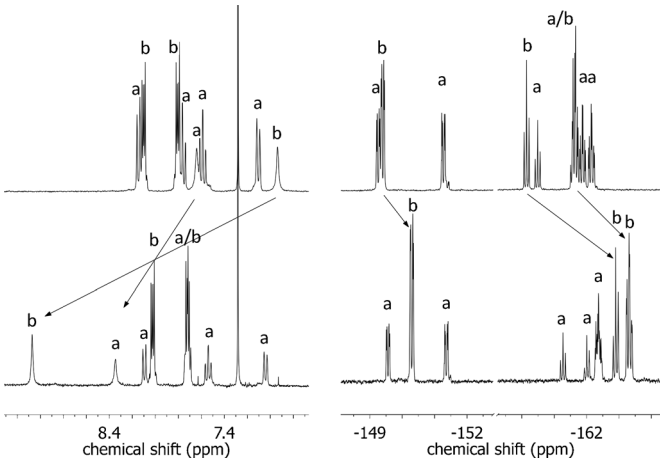

Figure 3. ^{1}H (left) and ^{19}F NMR spectra (right) of A^F measured in $CDCl_3$ before (top) and after (bottom) the addition of approximately ten equivalents $(Bu_4N)Br$. Signals labeled "a" and "b" are assigned to the *E*,*Z* and *Z*,*Z* isomers, respectively (compare Scheme 3).

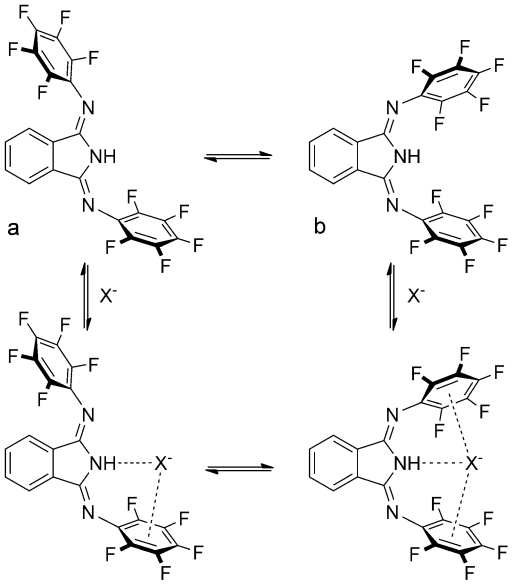

Scheme 3. Isomeric equilibrium between the *E*,*Z* (a) and *Z*,*Z* (b) forms of A^F in solution and their binding of halide anions X^-.

Addition of halide salts led to considerable shifts for the NH proton signals of both isomers as well as for the ^{19}F NMR resonances, more so for the *Z*,*Z* isomer than for the *E*,*Z* isomer. In addition, the *Z*,Z versus *E*,*Z* equilibrium is shifted towards the *Z*,*Z* form (Scheme 3, Figure 3; roughly a 1.5:1 *Z*,*Z* to *E*,*Z* ratio after addition of 10 equiv $(Bu_4N)Br$ in $CDCl_3$). Although a significant excess of halide salt was added to the solution, no complete conversion to the *Z*,*Z*-isomer was achieved. Thus, although receptor A^F shows a promising potential to bind anions, the complex equilibria in solution make further investigations and analysis of this system exceedingly cumbersome.

Slow diffusion of hexane into a solution of the receptor A^F in chloroform with an excess of either $(Me_3PhN)Cl$ or

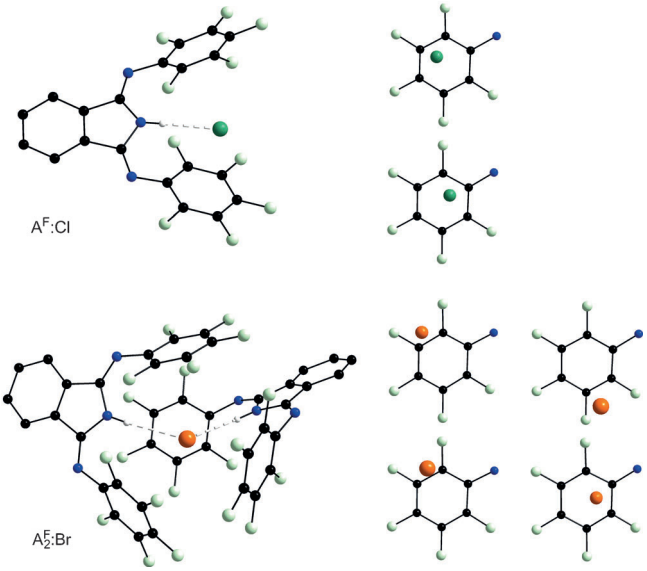

Figure 4. Molecular structures of $(Me_3PhN)[A^F{:}Cl]$ (top) and $(Ph_4P)[A_2^F{:}Br]$ (bottom). To visualize the position of the anions relative to the C_6F_5 flaps, the top view of each arene plane is depicted next to the structures. Cations and hydrogen atoms except for the NH proton are omitted for clarity.

$(Ph_4P)Br$ gave crystalline material that was analyzed by X-ray diffraction. The molecular structures of the anionic host–guest complexes of the salts $(Me_3PhN)[A^F{:}Cl]$ and $(Ph_4P)[A_2^F{:}Br]$ are shown in Figure 4.

The obtained structures of $A^F{:}Cl^-$ and $A_2^F{:}Br^-$ both show the halide located between the perfluorated flaps of the receptor A^F and hydrogen bonded to its central NH group (d(N···Cl) = 3.18 Å in $A^F{:}Cl^-$, d(N···Br) = 3.41/3.36 Å in $A_2^F{:}Br^-$) as anticipated beforehand. With chloride, A^F forms the expected 1:1 complex, whereas two A^F receptor molecules wrap around the bromide in $A_2^F{:}Br^-$, likely because of the larger size of bromide. In order to evaluate the two structures with respect to their anion–π interactions, the location of the anions relative to the C_6F_5 planes and their distances to either the center (d(X–centroid)) or the plane (d(X–plane)) of the arene were considered. In case of $A^F{:}Cl^-$ the chloride is located roughly above the center of the arene rings (Figure 4 top) with rather short distances d(Cl–centroid) = 3.28–3.35 Å and d(Cl–plane) = 3.28–3.30 Å. These values lie well within the typical range of anion–π interactions.[16a] For $A_2^F{:}Br^-$ the offset from the normal to the center of the arene ring is more pronounced and the bromide in most cases is located above a C–C bond, hence the interaction is best described as being of the η^2-type mode.[16a] Still, the distances are rather short and are found in the ranges d(Br–centroid) = 3.53–3.66 Å and d(Br–plane) = 3.27–3.46 Å, suggesting favorable anion–π interactions. The four C_6F_5 flaps in $A_2^F{:}Br^-$ wrap around the central bromide in a roughly tetrahedral arrangement, though the angle N···Br···N deviates from linearity (128°).

The related receptor A^N, on the contrary, gave a very simple ^{1}H NMR spectrum showing only one set of signals with a deshielded NH proton, and no further isomers

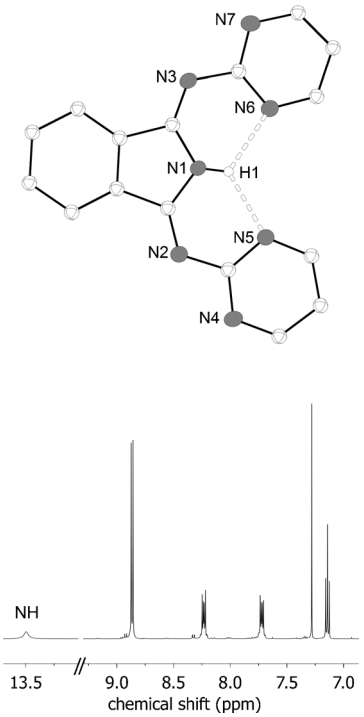

Figure 5. Molecular structure of A^N and its ^1H NMR spectrum measured in $CDCl_3$. Hydrogen atoms except for the NH proton are omitted in the structure.

(Figure 5). In this case the addition of either $(Bu_4N)Cl$ or $(Bu_4N)Br$ or other halide salts had no effect on the NMR chemical shifts, suggesting that A^N does not bind any anions. A rationalization is provided by the crystal structure, which clearly shows two strong intramolecular NH···N interactions (d(H···N) = 2.09/2.19 Å). This bifurcated hydrogen bond not only prevents *E*/*Z* isomerism, but seems to be so strong that neither solvent nor anions have any significant effect.

Type-B receptors: In the case of receptor B^F, because of the rigidity of the carbazole-based scaffold, isomerism cannot take place and the receptor is highly preorganized. Indeed, the neutral B^F showed a pronounced ability of binding halide anions as reflected by characteristic changes in the ^1H and ^{19}F NMR spectra upon addition of either $(Bu_4N)Cl$ or $(Bu_4N)Br$ (Figure 6). Unfortunately, all attempts to crystallize the anion-containing host–guest complexes B^F:X^- were unsuccessful.

Job plots for receptor B^F with Cl^- and Br^- showed a 1:1 stoichiometry in all solvent systems used in this work, namely CD_2Cl_2, CD_3CN, C_6D_6, and $[D_8]$THF (see Figure 7 top, and the Supporting Information). Titration experiments for each combination of anion and solvent were performed, monitoring the shifts of the *p*-F and NH signal as a function of the amount of anions added (Figure 7 bottom).

The obtained titration curves were then fitted with nonlinear and linear regression methods to extract the binding constants (see the Supporting Information for details). The resulting K_a values derived from Scatchard plots are listed in Table 1.

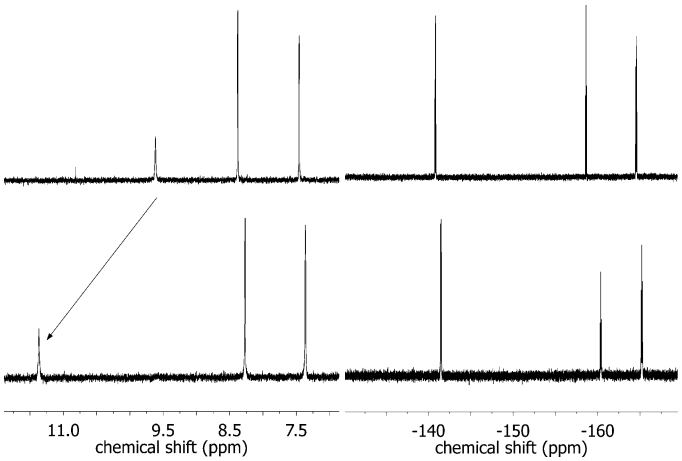

Figure 6. ^1H (left) and ^{19}F NMR (right) spectra of receptor B^F in $[D_8]$THF before (top) and after (bottom) addition of approximately three equivalents of $(Bu_4N)Br$.

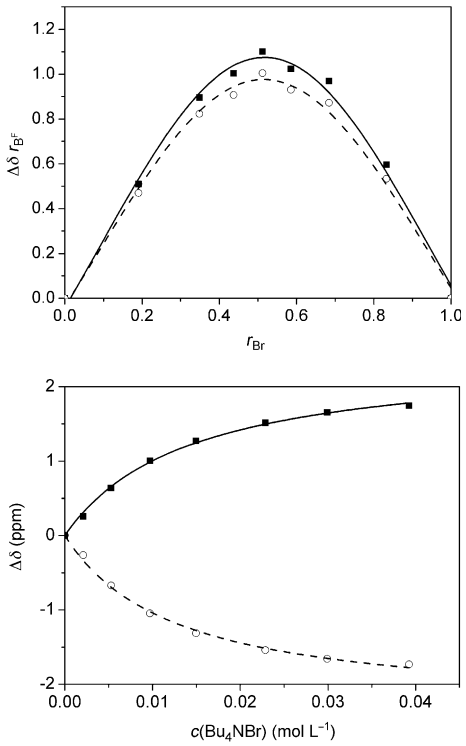

Figure 7. Job plot (top) and titration curve (bottom) of receptor B^F and $(Bu_4N)Br$ in $[D_8]$THF (■ = NMR signal of the NH group, ○ = NMR signal of the *p*-F).

Table 1. Association constants K_a [M^{-1}] for the 1:1 complexes of receptor B^F with Cl^- or Br^- in different solvents.

	CD_2Cl_2	CD_3CN	C_6D_6	$[D_8]$THF
B^F:Cl^-	4.1 ± 0.4	12.0 ± 0.7	(9.6 ± 4.6) × 10^2	(5.0 ± 2.5) × 10^2
B^F:Br^-	2.8 ± 0.2	6.6 ± 0.4	(4.4 ± 2.9) × 10^2	(2.8 ± 1.0) × 10^2

In all solvents the binding constants are higher for Cl^- than for Br^-, roughly by a factor of two. Although this general trend is expected,[15] the difference in the K_a values for Cl^- and Br^- may also reflect the better fit of the smaller Cl^-

into the highly preorganized cleft between the two arenes of the receptor. Association constants in CD_2Cl_2 and CD_3CN are quite small and the halide binding abilities of B^F are rather weak ($K_a = 12.0\,M^{-1}$ for B^F:Cl^- in CD_3CN, corresponding to $\Delta G = -6.1\,kJ\,mol^{-1}$), which may possibly reflect competing interactions of the solvent with the NH unit of the receptor as well as good solvation of the anions in the polar solvent CD_3CN. On the contrary, in C_6D_6 or $[D_8]THF$, where the halide salts $(Bu_4N)X$ are poorly soluble, the interaction of the anions with the receptor is more favored ($K_a = 960\,M^{-1}$ for B^F:Cl^- in C_6D_6, corresponding to $\Delta G = -16.7\,kJ\,mol^{-1}$). It is interesting to note that a surprisingly high association constant in the polar solvent CD_3CN was found for *N*,*N*′-(1,2-phenylene)-bis(pentafluorobenzamide) and chloride ($K_a \approx 3500\,M^{-1}$),[15] likely because of the presence of two N–H···Cl hydrogen bonds. To assess the individual contributions of N–H···X hydrogen-bonding and the anion–π interaction for the synergetic halide binding by the preorganized receptors A^F and B^F, detailed computational studies have been performed (see the following section).

Receptor B^H with phenyl flaps was synthesized to experimentally evaluate the effect of the electron-deficient C_6F_5 rings and their anion–π interactions. Titration of B^H with solutions of $(Bu_4N)Cl$ or $(Bu_4N)Br$ indeed showed no shifts of the NMR signals, neither for the NH nor the phenyl flaps (see the Supporting Information). Obviously, the attraction between the halide anion and the π-clouds of the phenyl flaps is too weak (or is even repulsive) and not competitive with the solvent. Electron-deficient arene rings are needed to enhance the interaction.

Computational results: In order to gain a deeper insight into each system, we have performed a series of computational structure calculations. The structures of the receptor system A^F both in its free form as well as interacting with chloride and bromide ions, A^F:X^- ($X = Cl^-$, Br^-), were optimized at the B3LYP-D3/def2-TZVPP level of theory,[22] all of them in the *Z*,*Z* conformation. The obtained structures of the anion–receptor adducts are shown in Figure S1 in the Supporting Information. Superposition plots of the structures of A^F:Cl^- determined by X-ray crystallography and computationally are provided in Figure S2 in the Supporting Information, revealing a very good agreement except for the rotational position of the C_6F_5 rings.

Only minor changes are observed on almost all atoms when comparing the computed structures of the free receptor with those of the host–guest complexes A^F:X^- ($X^- = Cl^-$, Br^-). The only exception is for the NH upon hydrogen binding to the anion, which moves out of the isoindole ring plane, directed towards the halide ion. Furthermore, the N–H bond length is slightly lengthened, from 1.004 to 1.064 and 1.049 Å, for A^F:Cl^- and A^F:Br^-, respectively. The effects of the hydrogen bond are visible in both the distance and the bending angle. To better illustrate this latter effect, superposition plots of the structure of receptor A^F with the adducts A^F:Cl^- and A^F:Br^- are shown in Figures S3 and S4 in the Supporting Information, respectively. The d(N···X) (X = Cl, Br) values are 3.016 and 3.230 Å, respectively, which are somewhat shorter than in the X-ray structures.

As mentioned above, the geometry of the receptor is only slightly affected by the coordination. The distance between both ring flaps (measured as the distance between both centers of mass) are 6.654, 6.166, and 6.641 Å, for A^F, A^F:Cl^- and A^F:Br^-, respectively. Even more, the tilted angles of the flaps with respect to the isoindolin plane change from 50.8/48.6° for A^F to 52.9/48.8° for the complex with either anion. Therefore, only in the case of the chloride do the rings move closer, possibly to enhance the interaction between the rings and the halide anion.

We have studied the energetics for the formation of host–guest complexes by computing the interaction energy (ΔE_{int}), the deformation energy of the receptor (ΔE_{def}), and the binding energy ($\Delta E_{bind} = \Delta E_{def} + \Delta E_{int}$). The deformation energy is the energy required to distort the free receptor into the geometry observed in the complex. In this regard, we have improved the energy obtained by carrying out single-point calculations at the DF-LMP2 level of theory,[23a–c] with the cc-pVTZ basis set for the hydrogen atoms and aug-cc-pVTZ for all remaining elements.[24] The basis set will be referred to as AVTZ for convenience. Because density-fitting approximations have been used throughout, we will also drop the "DF" prefix. The values are given in Table 2.

Table 2. Binding (ΔE_{bind}), interaction (ΔE_{int}) and deformation (ΔE_{def}) energy values (in [$kJ\,mol^{-1}$]) for the receptors A^F and B^F with chloride and bromide ions.

	B3LYP-D3			LMP2		
	ΔE_{bind}	ΔE_{def}	ΔE_{int}	ΔE_{bind}	ΔE_{def}	ΔE_{int}
A^F:Cl^-	−183.2	13.7	−196.9	−171.6	6.7	−178.3
A^F:Br^-	−152.3	10.2	−162.5	−152.8	5.0	−157.8
B^F:Cl^-	−178.2	9.7	−187.9	−160.1	12.4	−172.5
B^F:Br^-	−148.6	7.7	−156.3	−145.9	8.3	−154.2
A^F_2:Cl^-	−336.6	8.1/7.5	−352.2	−338.6	4.7/6.1	−349.4
A^F_2:Br^-	−287.9	7.1/5.8	−300.8	−293.1	2.6/3.2	−298.9

The LMP2/AVTZ and B3LYP-D3/def2-TZVPP energies are in relatively good agreement, showing the same trends in interaction strengths. The binding energies obtained are in the range expected for receptors with electron-deficient aromatic rings.[25] Comparing the halides, the binding energies with receptor A^F are somewhat larger in the case of Cl^-, by about 30.9 and 18.8 $kJ\,mol^{-1}$ for B3LYP-D3 and LMP2, respectively. The deformation energies are small, as expected in view of the only slight changes to the conformation. The small structural changes between the free receptor and the receptor–anion systems as well as the computed ΔE_{def} values confirm the compounds as suitably preorganized clamps for anion binding. The values in Table 2, however, give little information about the existence of anion–π interactions, and their weight in the total interaction. To investigate this effect, we have carried out calculations in model

systems, examining in greater detail the interaction between an anion and the fluorinated rings.

As a model system for the interaction of the flaps, we have used two pentafluorobenzene rings. The attractive interaction of the halide with electron-deficient aromatic rings has been a subject of several previous computational studies.[5c,13,26] Among them, it has been demonstrated that the strength of the anion–π interaction and its contributions to the interaction energy, namely electrostatic, induction, and dispersion, sharply depend on the quadrupole moment and the molecular polarizability values of the aromatic compound.[5c,d,27] On this ground, we opted for a pentafluoro-substituted benzene to mimic the former properties of the flaps of the receptor,[28] as the dipole moment can strongly influence the interaction with the anion. We have also kept in our calculations the orientation of the hydrogen bond as close as possible to what should be observed in the receptor.[16b,29] Because we are interested in the study of a receptor class (not a single compound), the relative orientation of the rings is a factor which has to be taken into account, given it may vary depending on the compound and upon coordination.[1d] We have considered two cases. In a first series of calculations, the pentafluorobenzene rings are placed parallel, with the anion in the middle (similar to a sandwich complex). In this case, the halide is located above the rings centroids. The potential energy plot is generated by a symmetric displacement of the rings, away from the halide (Figure 8). Furthermore, we have considered a bent orientation at 150° for the angle $ring_{centroid}$-X-$ring_{centroid}$, closely reproducing the orientation of compound $A^F{:}X^-$, and also the tilted angles of 58/58° from the parallel case. The displacements are made along the vector joining the halide and the geometric center of the ring (see Figure 8 for the representation). In this case, the halide is offset relative to the rings centroids, with the projection points changing with the varying distance. The potential energy curves for the chloride and bromide ions in the "parallel model" are given in Figures 8 A and B, respectively. In both cases, the reference is given by the LCCSD(T0)/AVTZ values.[23d] The SCS-LMP2/AVTZ[30] curves are almost coincident to the latter, whereas LMP2/AVTZ slightly overestimates the interaction. This is expected, because MP2 tends to overestimate the dispersion interactions.[31] The curves for the halides are rather similar, with comparable well depths (in numbers −85.3 and −71.6 kJ mol^{-1} at the LCCSD(T0)/AVTZ level of theory), but a shorter equilibrium distance in the case of Cl^- compared to Br^- (3.3 vs. 3.5 Å). These distances are in the range of those reported in the literature for 1:1 anion–π complexes,[26d,32] and they are in very good agreement with values found experimentally for $A^F{:}Cl^-$.

The effect of correlation is given by the difference of the calculated curves to the HF curve. It is evident that the systems interact even at an uncorrelated level, which is caused by electrostatic effects. For instance, when the anion is a chloride, the value at the equilibrium distance predicted by HF (3.5 Å) is −61.9 kJ mol^{-1} whereas for bromide (3.8 Å) it is −53.1 kJ mol^{-1}. The correlation energy contribution to the interaction predicted at the LMP2 level is about 45% for chloride and 50% for bromide. The correlation energy values computed for each anion are −42.4 and −43.6 kJ mol^{-1} for chloride and bromide, respectively. The values are quite similar as a result of a balance between the shorter interaction distances for chloride on the one hand and the larger polarizability of bromide on the other hand. In order to better understand the role of correlation effects,

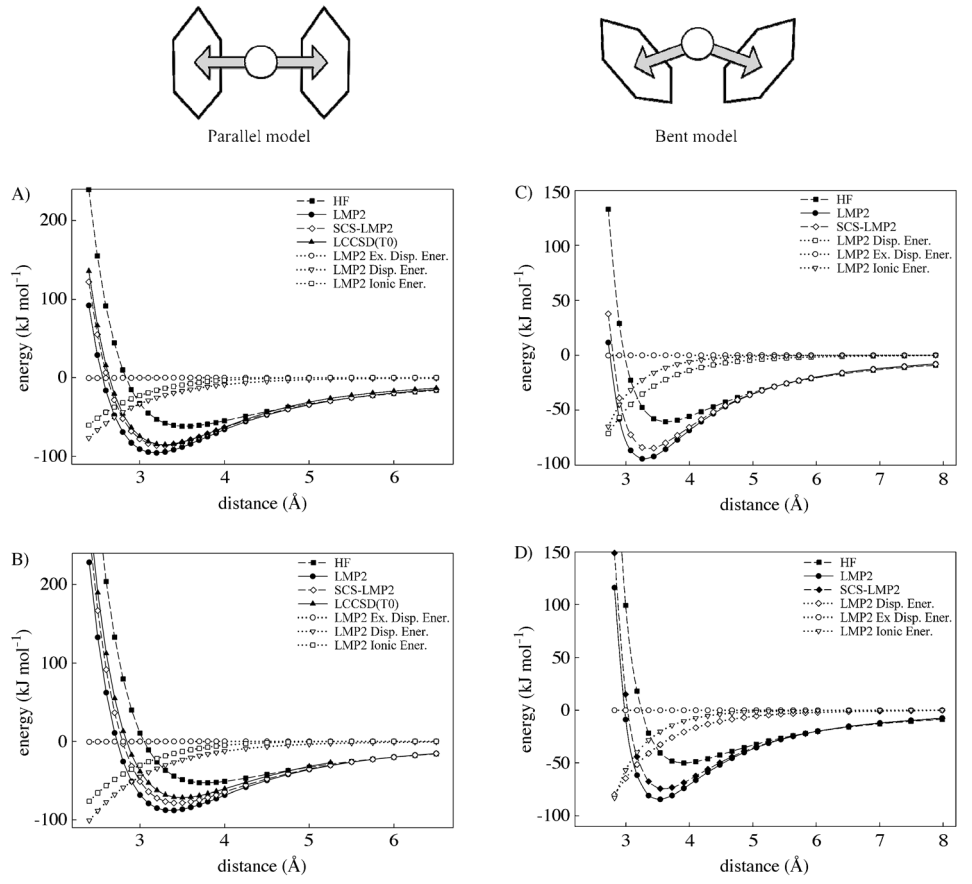

Figure 8. Potential energy curves of the parallel model with A) Cl^- and B) Br^- ions and of the bent model with C) Cl^- and D) Br^- ions. The energy values are given as a function of the distance between the center of the ring and the halide anion.

we have carried out a decomposition of the LMP2 energy. The local character of occupied and virtual orbitals in the local correlation treatments offers the possibility to dissect intramolecular effects (double excitations from occupied orbitals of one unit into virtual orbitals of the same unit) from intermolecular ones (excitations involving orbitals from both units).[33] Additionally, the intermolecular correlation effects can be decomposed according to different excitation classes: dispersion effects originate from simultaneous monoexcitations at each unit, exchange–dispersion is similar but the monoexcitations are from the occupied space of one unit to the virtual space of the other and vice versa; ionic contributions come from monoexcitations from the occupied space of both units into the virtual space of only one of them. The different classes have been discussed in detail by Schütz et al.[33] In Figures 8A and B, together with the energy curves, each intermolecular contribution term is also displayed as a function of the distance between the center of the ring and the halide anion, corresponding to anion–ring interactions. These curves show a continuous favorable interaction with decreasing distances. As has been expected, the main contributions to the interaction from the correlation energy are linked to dispersion (58–63%) and ionic excitations (36–37%) whereas the exchange–dispersion effect is negligible. These observations are in accordance with previous reports on anion–π interactions.[5d,13b,26h,34] It is important to stress that the dispersion and ionic effects significantly contribute to a shorter contact, in both cases contracting the equilibrium distance by about 0.3–0.4 Å. This is far from being a minor effect, and it cannot be attributed to classical electrostatic interactions. However, this is in disagreement with another theoretical study, which connected the stabilization of such systems to a substituent–anion electrostatic interaction.[35] Such energy terms are included solely in the HF contribution.

The results obtained for the bent model show relatively similar profiles (Figures 8C and D). The minimum distances are practically coincident with those derived from the parallel model, namely 3.2–3.4 Å. This indicates that the orientation of the rings plays a relatively small role and that one can extrapolate some of the findings in the parallel model to the compound structures, at least for 150° of the bent angle $ring_{centroid}$-X-$ring_{centroid}$.

These results can help us to better understand the structures of receptor A^F with the different anions. The curves in Figures 8A and C show that the optimal distance for the $Cl^-\cdots\pi$ interaction would be 3.2 Å regardless of the disposition of both rings (the bent angle) at the LMP2 level of theory. Strikingly, the anions stay out of the isoindole plane of the molecule instead of penetrating deep into the cavity. Albrecht et al. and Hay et al. (among others) have addressed this issue in some experimental and computational systematic studies on differently substituted electron-deficient arenes. Their results revealed the flexibility in the position of the anion over the rings. These positions can be controlled by a hydrogen-bond donor directing substituent, such as C–H and N–H bonds.[3c,12a,15,16,29,36] The N–H$\cdots X^-$ interaction in A^F:Cl^- keeps the chloride ion close to the rim of the arene, as evidenced by the offset distances (Figure 8). Moreover, the relative rigidity of the receptor flaps hinders the perfect fit into the host cavity. The Wiberg bond order of the linking C–N bonds has been computed within the natural bond order (NBO)[37] framework, at the B3LYP/def2-TZVPP level of theory, giving values of around 1.1 au, which indicate a weak double-bond character (see Table S5 in the Supporting Information for more information). The anion–π interactions nevertheless are enhanced by bringing the two rings together. From the curve in Figure 8C a gain of about 10 kJ mol^{-1} can be estimated. In the case of Br^-, no such displacement takes place because the free state has an optimal distance for the contact.

Insight into the nature of the binding energy was obtained by evaluating the weight of the principal interactions in the binding of the host–guest complex A^F:X^-, namely the hydrogen bond, dispersion, and ionic correlation energies. The values are gathered in Table 3. An approach to the nature of the N–H$\cdots Cl^-$ interaction was reached by computing the charge transfer (q_{CT}) from the halide to the N–H bond. The NBO method was used to estimate the extent of this leading interaction;[37] NBO calculations were carried out at the B3LYP/def2-TZVPP level of theory.

Table 3. Partitioning of the LMP2 interaction energies (in [kJ mol^{-1}]) and the natural population analysis (NPA) charge transfer (q_{CT})[a,b] for the anion–receptor interactions in all A^F and B^F anion adducts. The different values per entry refer to the contribution of each separated ring.

Compound	ΔE_{int}	ΔE_{disp}	ΔE_{ionic}	$\Delta E_{disp}+\Delta E_{ionic}$	q_{CT}
A^F:Cl^-	−178.3	−14.8/−15.8	−7.5/−8.6	−22.3/−24.4	0.156
A^Fm:Cl^-[c]	−91.4	−14.9/−15.3	−9.1/−8.8	−24.0/−24.1	
A^F:Br^-	−157.8	−15.8/−16.8	−8.2/−9.1	−24.0/−25.9	0.131
A^Fm:Br^-[c]	−81.9	−14.3/−15.3	−8.3/−9.2	−22.6/−24.6	
B^F:Cl^-	−172.5	−16.0/−18.9	−8.6/−9.8	−24.7/−28.8	0.121
B^Fm:Cl^-[c]	−93.6	−15.1/−15.0	−8.8/−8.4	−24.0/−23.4	
B^F:Br^-	−154.2	−17.0/−20.8	−9.6/−11.5	−26.6/−32.3	0.100
B^Fm:Br^- [c]	−87.3	−16.1/−16.3	−9.3/−9.2	−25.4/−25.4	
A^F_2:Cl^-	−349.4	−10.9/−16.1/−11.2/−15.1	−4.9/−7.5/−5.07/−6.6	−15.8/−23.7/−16.3/−21.7	0.183
A^F_2:Br^-	−298.9	−16.0/−15.9/−17.6/−13.9	−8.4/−8.2/−9.3/−6.5	−24.4/−24.1/−26.9/−20.4	0.141

[a] NBO calculations were computed with B3LYP/def2-TZVPP. [b] Charge transfer is defined as $q_{CT}=q_X(\text{complex})-q_X(\text{isolated})$. [c] A^Fm and B^Fm refer to the flap model, see the main text.

Regarding the decomposition of the LMP2 energies, only dispersion and ionic correlation interactions can be separated from the total interaction. These values are also given in Table 3 for a better comparison, together with the sum of the two previously mentioned contributions. In the case of the complete complexes A^F:Cl^- and A^F:Br^-, the ΔE_{disp} and the ΔE_{ionic} values were computed by dissecting the energy

terms between the orbitals in the rings and the anions (Pipek-Mezey-localized). As it can be seen, the dispersion interactions contribute with 17 and 21%, respectively, to the binding energy for A^F:Cl^- and A^F:Br^-. In the case of the ionic interaction energy the contribution is even lower, being roughly 10% of the total energy for both complexes. It is worth noting that the total correlation energy values for both anions are close, that is, 46.7 kJ mol^{-1} for Cl^- and 49.9 kJ mol^{-1} for Br^-, pointing out that the differences in the binding energy for each halide are already contained in the reference energy. It is remarkable that the contributing terms of the LMP2 energies computed here are coincident with those computed for the parallel and bent curves, supporting the good representation acquired by the model used. Although electrostatic interactions dominate the coordination of the halides to the compounds under study,[1d,2b,7b] a significant part of the interaction is due to dispersion. Furthermore, the bent structure of the rings is a direct consequence of correlation effects between the diffuse electron cloud of the anion and the ring system, shifting the interaction potential of about 0.3–0.4 Å to smaller contact distances.

On the other hand, the values of the interaction NH···X^- seem to be strong contributors to the binding process. The values shown here are within the range expected, given the electron-withdrawing character of the perfluoroarene substituents of the isoindole fragment.[32,36c,38] Thus, in order to get an idea of the importance of N–H bonds, we have built a simplified model based on the good representations of the pentafluorobenzene, keeping the position of the flaps as they are in the host–guest complex but erasing the isoindole moiety (or the carbazole ring); these model structures are referred to in Table 3 as A^Fm:X^- (or B^Fm:X^-). The binding energy obtained in this way revealed that the anion–π interaction contributes at least 53% of the total binding energy in A^F:X^- and B^F:X^-, whereas the remainder is due to the NH···X^- hydrogen bonds. The energies obtained reveal a pronounced difference of the interaction depending on the nature of the halide, that is, 86.9 and 75.9 kJ mol^{-1} for chloride and bromide ions, respectively. In the same way the amount of charge transfer (CT) is higher for Cl^- than Br^-, which is in good agreement with previous reports.[32] The CT is in the order of 0.1 electrons, which is mainly due to the NH···X^- bond.

It was also possible to obtain stable minima geometries for the A^F_2:X^- complexes. Figure 9 shows superposition plots comparing the computed A^F_2:X^- complexes (for $X^- = Cl^-$ and Br^-) with the free receptor structure (see Figures S5–S7 in the Supporting Information for further details).

The interaction energies for the complexes A^F_2:X^- are given in Table 2. From a straightforward comparison between the interaction energies in the case of the monomers and the dimers, one can observe that there is no additivity effect on the binding energy. Even more, the total dimer interaction is lower than the sum of two monomers by about 29.8 and 16.7 kJ mol^{-1} for Cl^- and Br^-, respectively (B3LYP-D3). Non-additivity effects on 3:1 complexes have been attributed to the extra interaction between arene rings.[25] In the present case, this effect could be due to the fact that each A^F molecule hinders the other in its interaction with the anion. This effect is higher for chloride complexes because each receptor ring has to move closer to the halide, as is reflected by the structural changes upon dimer formation. For instance, the hydrogen bonds are longer in the 2:1 complex than in the 1:1 complex by 0.070 Å for Cl^- and by 0.126 Å for Br^-, and the angles of the flap (C-N-C) are widened by about 7 and 2° for Cl^- and Br^-, respectively. The radii of the chloride and bromide ions seem to be somewhat small for the pocket formed between the two host molecules; consequently they interact strongly with two of the arenes and weakly with the remaining ones. The data in Table 3 clearly show the different strength of the anion–π interaction with the four flaps, and also that they are on average slightly lower for the dimers than for the monomers. Bulkier receptor molecules might completely avoid dimer formation.

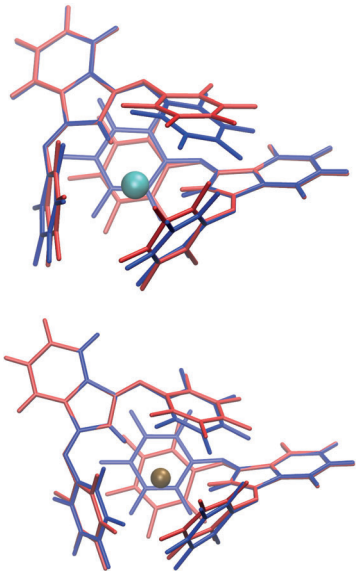

Figure 9. Comparison of the optimized geometries for the A^F_2:X^- adduct (in red) and the two overlapped relaxed A^F monomers (in blue) in the case of X^- = chloride (top) and for X^- = bromide (bottom). For further views see the Supporting Information.

As in the case of complexes A^F:X^-, the structures of compounds B^F:X^- have been optimized and their interaction energies are compared in Table 2. The B3LYP-D3/def2-TZVPP geometries are given in Figure 10 (and in Figure S8 in the Supporting Information).

Upon halide binding these structures show a larger difference in the ring distances (see Table S4 in the Supporting Information). When compared to compound A^F, the rings move closer together and the difference between the two halides is accentuated. As can be seen in Figure 10 the main difference between the relaxed geometry of receptor B^F and the one in the B^F:X^- complexes is due to the tilted angle of the flaps, the change is from 43.8/48.9 to 63.6/71.9 and 62.6/72.0° for chloride and bromide (in that order). The better fit

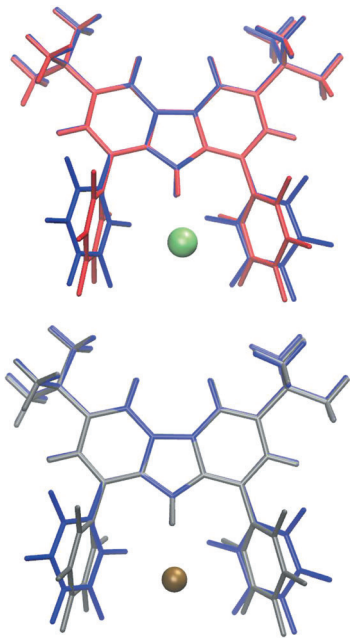

Figure 10. Superposition plots with a least-square fit of the computed structures for the free B^F receptor and its complexes with chloride (top) and bromide (bottom). The structure in blue is the free receptor and the structures in red or gray are the structures of the adducts. The optimizations were performed at the B3LYP-D3/def2-TZVPP level of theory. For further views see the Supporting Information.

into the host pocket is a consequence of a certain freedom in the C–C bond linker rotation; the computed Wiberg bond orders reveal a single-bond character as expected (Table S5 in the Supporting Information). However, as shown in Table 2, this has no reflection in the interaction energies, which are lower than the energies obtained with the receptor A^F. The deformation energies are very similar. A better interpretation can be drawn from the decompositions of the energies given in Table 3. At the first glance it becomes obvious that the better fit means a small increase in the anion–π interaction for receptor B^F. Comparison of the modeled flaps leads to an increase of this interaction of about 2.2 and 5.4 kJ mol^{-1} with Cl^- and Br^-, respectively. In contrast, the hydrogen-bond interaction is strongly reduced in compound B^F, and seems to be the mandatory interaction. Thus, the charge transfer is lower for both halide anions. This result follows the trend dictated by the acidity of the heterocycle.

Conclusion

We have presented a combined experimental and computational study of two novel neutral anion receptors, that is, compounds A^F and B^F, which are highly preorganized for accommodating halide ions in a cleft between two pentafluorophenyl rings. The propensity of the receptors to bind chloride and bromide was confirmed in solution through NMR spectroscopy and in the crystal structures of several host–guest complexes—the latter are rare examples of crystallographically characterized anion–π complexes with uncharged receptors. The anion affinity is a result of favorable anion–π interactions with the pentafluorophenyl groups in complexes $A^F{:}X^-$ and $B^F{:}X^-$, supported by the more directional hydrogen bond to the NH group in the central skeleton, and consequently the non-fluorinated derivatives A^N and B^H are not capable of hosting any halide ions under the conditions used in the present work.

In the case of $A_2^F{:}Br^-$, the anion is embraced by two host molecules, possibly due to the larger size of the anion and a slightly larger opening of the flanking rings. The relative position to the C_6F_5 planes is within typical ranges for anion–π interactions. In $A_2^F{:}Br^-$ the anion is somewhat displaced to the edge of the ring, forming an η^2-type interaction. Binding constants have also been measured for compound B^F, comparing the affinity to chloride and bromide ions. The expected trends are observed, with chloride revealing a stronger binding and with lower affinities for increasing solvent polarity.

Detailed electronic structure calculations have been carried out on the compounds in order to obtain further insight into the specific anion interactions. Through the use of a model consisting of two pentafluorobenzene rings, we were able to decompose the interaction between the receptors and the anions. Comparison of the interaction energies in the full host–guest complex and the model shows that direct anion interactions with the flanking electron-deficient arenes can contribute as much as half of the total effect. The adequacy of our model has been confirmed by analyzing different conformations and comparing the correlation energy contributions from localized orbitals found in the arene flaps and the two isolated rings. Through the use of local orbital spaces, we were also able to dissect the effect of electronic correlation in the structure of the host–guest complexes. Dispersion interactions contribute as much as 20% to the stabilization energy, with a slightly larger contribution in the case of bromide. All of these results underline the importance of the electron-deficient arenes in promoting the anion binding. Low deformation energies upon complexation show that the synthesized molecules are in fact close to an ideal conformation to trap the halides within their cleft. This observation is also supported by comparing the optimal anion–ring distances in the potential energy profiles and the distances measured both in the structures determined crystallographically and optimized computationally.

Overall this study shows that efficient anion binding can be achieved in well preorganized receptors that exploit the synergetic effect of directional hydrogen-bonding and anion–π interactions. The latter contribute significantly to the overall binding energies, confirming that anion–π interactions are useful instruments in the design of uncharged anion receptors that do not rely on salt bridges and require only few complementary interactions, such as a single N–H···X^- hydrogen bond in the present case.

Experimental Section

Physical measurements: NMR spectra were recorded on an Advance III 300 MHz spectrometer (Bruker) by using the indicated deuterated solvent as internal standard. EI-MS spectra were recorded on a Finnigan MAT 8200 spectrometer and ESI-MS spectra were recorded on an Applied Biosystems API 2000 spectrometer. Experimental procedures and data analysis for the Job plots and titration experiments are provided in the Supporting Information.

X-ray crystallography: X-ray data were collected on a STOE IPDS II diffractometer with an area detector (graphite monochromated $Mo_{K\alpha}$ radiation, $\lambda = 0.71073$ Å) by using ω scans at 133 K (Table S6 in the Supporting Information). The structures were solved by direct methods and refined on F^2 by using all reflections with SHELX-97.[39] Most non-hydrogen atoms were refined anisotropically. Most hydrogen atoms were placed in calculated positions and assigned to an isotropic displacement parameter of 1.2/1.5 U_{eq} (C or N). The hydrogen atoms H1 and H2 in A_2^F:Br^- and A^N were refined without any restraints or constraints; a fixed isotropic displacement parameter of 0.08 Å^2 for the nitrogen-bound hydrogen atoms was applied in case of B^F:DMSO, A^F:Cl^-, and B^F. Disordered DMSO solvent molecules are present in A^F:DMSO (occupancy factors: 0.816(3)/0.184(3)) and B^F:DMSO (fixed occupancy of 0.5 and 0.2818(17)/0.2182(17)), and a disordered toluene molecule in B^F (fixed occupancy of 0.5). One of the *t*Bu groups in B^F is disordered as well (occupancy factors: 0.747(4)/0.253(4)). EADP constraints (A^F:DMSO, B^F:DMSO), DFIX, SIMU, DELU, and ISOR restraints (B^F) were applied to model the disorder. Face-indexed absorption corrections were performed numerically with the program X-RED.[40]

CCDC-964440, -964441, -964442, -964443 -964444 and -964445 contain the supplementary crystallographic data for this paper. These data can be obtained free of charge from The Cambridge Crystallographic Data Centre via www.ccdc.cam.ac.uk/data_request/cif

Materials and synthetic procedures: All reactions were carried out under a nitrogen atmosphere. *n*-Butanol was dried over sodium to remove excess of water. Starting materials and solvents were purchased either from abcr, Sigma Aldrich, or Acros.

1,3-Bis(pentafluorophenylimino)isoindoline (A^F):[18a] Phthalonitrile (1.28 g, 10 mmol), pentafluoroaniline (3.66 g, 40 mmol) and $CaCl_2$ (0.05 g, 0.5 mmol) were heated to reflux in *n*-butanol (5 mL) for twenty days. After removal of the solvent, hexane was added to the residue. Filtration of the mixture gave a yellow solution. After removal of the solvent, the residue was purified through column chromatography (ether/hexane 1:1) yielding a pale yellow solid (1.08 g, 23%). ^{1}H NMR (300 MHz, $CDCl_3$): $\delta = 8.13$ (d, $J = 7.7$ Hz, 1H; H^a), 8.05–8.01 (m, 2H; H^b), 7.82–7.75 (m, 2H; H^b), 7.74 (td, $J = 7.6$, 0.7 Hz, 1H; H^a), 7.62 (s, 1H; NH^a), 7.57 (td, $J = 7.7$, 1.0 Hz, 1H; H^a), 7.08 (d, $J = 7.8$ Hz, 1H; H^a), 6.92 ppm (s, 1H; NH^b); ^{19}F NMR (282 MHz, $CDCl_3$): $\delta = -149.26$ (dd, $J = 23.0$, 5.8 Hz, 2F; F^a), −149.40 (dd, $J = 22.5$, 5.9 Hz, 4F; F^b), −151.13–−151.36 (m, 2F; F^a), −160.15 (t, $J = 21.5$ Hz, 2F; F^b), −160.49 (t, $J = 21.4$ Hz, 1F; F^a), −161.48–−161.76 (m, 3F; F^a, F^b), −161.88 (td, $J = 22.1$, 6.4 Hz, 2F; F^a), −162.15 ppm (td, $J = 21.4$, 5.4 Hz, 2F; F^a); MS (EI): *m*/*z* (%): 477 (100) $[M]^+$, 295 (47), 438 (32), 458 (89).

1,3-Bis(2-pyrimidylimino)isoindoline (A^N):[18] Phthalonitrile (0.64 g, 5 mmol), 2-aminopyrimidine (1.90 g, 20 mmol), and $CaCl_2$ (0.05 g, 0.5 mmol) were dissolved in *n*-butanol (5 mL) and heated to reflux for 21 d. After evaporation of the solvent first byproducts were removed through column chromatography (dichloromethane/methanol 19:1). To further purify the product, Kugelrohr distillation was utilized. The product was obtained as a yellow solid (0.1 g, 7%). ^{1}H NMR (300 MHz, $CDCl_3$): $\delta = 13.47$ (s, 1H; NH), 8.84 (d, $J = 4.8$ Hz, 4H), 8.26–8.16 (m, 2H), 7.75–7.65 (m, 2H), 7.12 ppm (t, $J = 4.8$ Hz, 2H); MS (EI): *m*/*z* (%): 301 (100) $[M]^+$, 79 (27), 207 (38), 222 (33).

3,6-Di-tert-*butyl-1,8-bis(perfluorophenyl)-9*H-*carbazole (B^F)*: The boronated precursor was synthesized following literature procedures.[19–20] 3,6-Di-*tert*-butyl-1,8-bis(4,4,5,5-tetramethyl-1,3,2-dioxaborolan-2-yl)-9*H*-carbazole **3** (2.18 g, 4.1 mmol) and $[Pd(PPh_3)_4]$ (94.8 mg, 0.8 mmol) were dissolved in toluene (500 mL). Ethanol (200 mL) and an aqueous solution of K_2CO_3 (2 M, 50 mL) were added and the mixture was degassed 3–5 times. Subsequently bromopentafluorobenzene (2 mL, 16.0 mmol) was added under a nitrogen atmosphere and the mixture was stirred at 90 °C for 16 h. The solvent was removed and the crude product was re-dissolved in dichloromethane (50 mL). After filtration over a short silica column the solvent was removed and the product was obtained as a white solid (2.14 g, 85%). Kugelrohr distillation of the crude product yielded white crystals, which were then used for further experiments. ^{1}H NMR (300 MHz, $CDCl_3$): $\delta = 8.24$ (d, $J = 1.7$ Hz, 2H), 7.45 (s, 2H), 7.40 (s, 1H; NH), 1.48 ppm (s, 18H); ^{13}C NMR (75 MHz, $CDCl_3$): $\delta =$ 143.49, 136.44, 126.78, 124.60, 118.29, 108.64, 34.96, 32.05 ppm; ^{19}F NMR (282 MHz, $CDCl_3$): $\delta = -139.80$ (dd, $J = 22.7$, 7.8 Hz, 4F), −154.31 (t, $J =$ 21.0 Hz, 2F), −161.02 ppm (td, $J = 22.3$, 7.6 Hz, 4F); MS (EI): *m*/*z* (%): 611 (46) $[M]^+$, 596 (100).

3,6-Di-tert-*butyl-1,8-diphenyl-9*H-*carbazole (B^H)*:[19,20] The synthesis was done as described for receptor B^F, but using four equivalents of bromobenzene instead. After removal of the solvent the solid was dissolved in dichloromethane/EtOH and left to crystallize at 8 °C. The product was obtained as pale yellow crystals (0.17 g, 70%, starting with 0.30 g (0.56 mmol) of **3**). ^{1}H NMR (300 MHz, $CDCl_3$): $\delta = 8.35$ (s, 1H; NH), 8.14 (d, $J = 1.8$ Hz, 2H), 7.75–7.63 (m, 4H), 7.60–7.46 (m, 6H), 7.41 (ddd, $J = 7.3$, 3.9, 1.3 Hz, 2H), 1.53 ppm (s, 18H); ^{13}C NMR (75 MHz, $CDCl_3$): $\delta = 141.97$, 138.61, 134.73, 128.18, 127.16, 126.30, 123.24, 123.00, 122.86, 114.60, 33.79, 31.05 ppm; MS (EI): *m*/*z* (%): 431 (79) $[M]^+$, 416 (100).

Computational details: All geometry optimizations were carried out by using the hybrid density functional B3LYP-D3[22a–c] with the basis set def2-TZVPP.[22d] The RIJCOSX method was applied to speed up the calculations.[41] The stationary points were located with the quasi-Newton algorithm by using redundant internal coordinates. Hessians were computed to determine the nature of stationary points. These theoretical calculations were performed with the ORCA program package.[42]

We performed single-point calculations on the B3LYP-D3-optimized structures with second-order local Møller–Plesset perturbation theory (LMP2)[23a–c] by employing the MOLPRO 2012.1[43] software program package. Density fitting (DF) approximations have been used in this local method.[23c] The aug-cc-pVTZ basis set was used for carbon, nitrogen, fluorine, chlorine, and bromine atoms whereas for hydrogen atoms the cc-pVTZ basis set was used.[24] In the density fitting calculations reported in this paper, we used the aug-cc-pVTZ/JKJIT and aug-cc-pVTZ/MP2FIT auxiliary fitting basis sets[44] in the DF-HF and DF-LMP2 calculations, respectively.

The LMP2 calculations were carried out by using Pipek-Mezey-localized orbitals.[45] The domains were determined with the use of natural population analysis (NPA) criteria, with $T_{NPA} = 0.03$.[46]

The NPA charge analysis[37a,c–e] and the reported Wiberg bond indices were computed by using the GENNBO 5.9 program.[47]

Acknowledgements

Financial support by the Georg-August-University is gratefully acknowledged. D.M.A. gratefully acknowledges a postdoctoral fellowship from ARCOIRIS Erasmus Mundus Action 2.

[1] a) B. L. Schottel, H. T. Chifotides, K. R. Dunbar, *Chem. Soc. Rev.* **2008**, *37*, 68–83; b) O. B. Berryman, D. W. Johnson, *Chem. Commun.* **2009**, 3143–3153; c) A. Robertazzi, F. Krull, E. W. Knapp, P. Gamez, *CrystEngComm* **2011**, *13*, 3293–3300; d) A. Frontera, P. Gamez, M. Mascal, T. J. Mooibroek, J. Reedijk, *Angew. Chem.* **2011**, *123*, 9736–9756; *Angew. Chem. Int. Ed.* **2011**, *50*, 9564–9583.

[2] a) B. P. Hay, R. Custelcean, *Cryst. Growth Des.* **2009**, *9*, 2539–2545; b) T. J. Mooibroek, C. A. Black, P. Gamez, J. Reedijk, *Cryst. Growth Des.* **2008**, *8*, 1082–1093.

[3] a) E. A. Meyer, R. K. Castellano, F. Diederich, *Angew. Chem.* **2003**, *115*, 1244–1287; *Angew. Chem. Int. Ed.* **2003**, *42*, 1210–1250; b) E. A. Meyer, R. K. Castellano, F. Diederich, *Angew. Chem.* **2003**,

115, 4254; *Angew. Chem. Int. Ed.* **2003**, *42*, 4120; c) B. P. Hay, V. S. Bryantsev, *Chem. Commun.* **2008**, 2417–2428.

[4] a) H.-J. Schneider, F. Werner, T. Blatter, *J. Phys. Org. Chem.* **1993**, *6*, 590–594; b) H. J. Schneider, *Angew. Chem.* **1991**, *103*, 1419–1439; *Angew. Chem. Int. Ed. Engl.* **1991**, *30*, 1417–1436; c) K. Hiraoka, S. Mizuse, S. Yamabe, *J. Phys. Chem.* **1987**, *91*, 5294–5297.

[5] a) M. Mascal, A. Armstrong, M. D. Bartberger, *J. Am. Chem. Soc.* **2002**, *124*, 6274–6276; b) I. Alkorta, I. Rozas, J. Elguero, *J. Am. Chem. Soc.* **2002**, *124*, 8593–8598; c) D. Quiñonero, C. Garau, A. Frontera, P. Ballester, A. Costa, P. M. Deyà, *Chem. Phys. Lett.* **2002**, *359*, 486–492; d) D. Quiñonero, C. Garau, C. Rotger, A. Frontera, P. Ballester, A. Costa, P. M. Deyà, *Angew. Chem.* **2002**, *114*, 3539–3542; *Angew. Chem. Int. Ed.* **2002**, *41*, 3389–3392.

[6] S. Demeshko, S. Dechert, F. Meyer, *J. Am. Chem. Soc.* **2004**, *126*, 4508–4509.

[7] a) Y. S. Rosokha, S. V. Lindeman, S. V. Rosokha, J. K. Kochi, *Angew. Chem.* **2004**, *116*, 4750–4752; *Angew. Chem. Int. Ed.* **2004**, *43*, 4650–4652; b) P. De Hoog, P. Gamez, I. Mutikainen, U. Turpeinen, J. Reedijk, *Angew. Chem.* **2004**, *116*, 5939–5941; *Angew. Chem. Int. Ed.* **2004**, *43*, 5815–5817; c) A. Frontera, F. Saczewski, M. Gdaniec, E. Dziemidowicz-Borys, A. Kurland, P. M. Deyà, D. Quiñonero, C. Garau, *Chem. Eur. J.* **2005**, *11*, 6560–6567; d) M. Mascal, I. Yakovlev, E. B. Nikitin, J. C. Fettinger, *Angew. Chem.* **2007**, *119*, 8938–8940; *Angew. Chem. Int. Ed.* **2007**, *46*, 8782–8784.

[8] S. Guha, S. Saha, *J. Am. Chem. Soc.* **2010**, *132*, 17674–17677.

[9] a) J. Mareda, S. Matile, *Chem. Eur. J.* **2009**, *15*, 28–37; b) A. Vargas Jentzsch, D. Emery, J. Mareda, P. Metrangolo, G. Resnati, S. Matile, *Angew. Chem.* **2011**, *123*, 11879–11882; *Angew. Chem. Int. Ed.* **2011**, *50*, 11675–11678; c) A. Vargas Jentzsch, A. Hennig, J. Mareda, S. Matile, *Acc. Chem. Res.* **2013**, DOI: 10.1021/ar400014r.

[10] a) D. Quiñonero, A. Frontera, P. M. Deyà in *Anion Coordination Chemistry*, Wiley-VCH, Weinheim, **2011**, pp. 321–361; b) H. T. Chifotides, K. R. Dunbar, *Acc. Chem. Res.* **2013**, *46*, 894–906.

[11] a) C. Estarellas, A. Frontera, D. Quiñonero, P. M. Deyà, *Chem. Asian J.* **2011**, *6*, 2316–2318; b) C. Estarellas, A. Frontera, D. Quiñonero, P. M. Deyã, *Angew. Chem.* **2011**, *123*, 435–438; *Angew. Chem. Int. Ed.* **2011**, *50*, 415–418.

[12] a) G. Gil-Ramírez, E. C. Escudero-Adán, J. Benet-Buchholz, P. Ballester, *Angew. Chem.* **2008**, *120*, 4182–4186; *Angew. Chem. Int. Ed.* **2008**, *47*, 4114–4118; b) P. Arranz-Mascarós, C. Bazzicalupi, A. Bianchi, C. Giorgi, M.-L. Godino-Salido, M.-D. Gutiérrez-Valero, R. Lopez-Garzón, M. Savastano, *J. Am. Chem. Soc.* **2013**, *135*, 102–105; c) P. Ballester, *Acc. Chem. Res.* **2013**, *46*, 874–884.

[13] a) C. Garau, A. Frontera, D. Quiñonero, P. Ballester, A. Costa, P. M. Deyà, *ChemPhysChem* **2003**, *4*, 1344–1348; b) C. Garau, A. Frontera, D. Quiñonero, P. Ballester, A. Costa, P. M. Deyà, *J. Phys. Chem. A* **2004**, *108*, 9423–9427.

[14] O. B. Berryman, F. Hof, M. J. Hynes, D. W. Johnson, *Chem. Commun.* **2006**, 506–508.

[15] M. Giese, M. Albrecht, T. Krappitz, M. Peters, V. Gossen, G. Raabe, A. Valkonen, K. Rissanen, *Chem. Commun.* **2012**, *48*, 9983–9985.

[16] a) M. Albrecht, C. Wessel, M. De Groot, K. Rissanen, A. Lüchow, *J. Am. Chem. Soc.* **2008**, *130*, 4600–4601; b) M. Giese, M. Albrecht, K. Wiemer, A. Valkonen, K. Rissanen, *New J. Chem.* **2012**, *36*, 1368–1372.

[17] M. Giese, M. Albrecht, K. Wiemer, G. Kubik, A. Valkonen, K. Rissanen, *Eur. J. Inorg. Chem.* **2012**, 2995–2999.

[18] a) W. O. Siegl, *J. Org. Chem.* **1977**, *42*, 1872–1878; b) D. M. Baird, K. Y. Shih, *Polyhedron* **1991**, *10*, 229–235.

[19] V. C. Gibson, S. K. Spitzmesser, A. J. P. White, D. J. Williams, *Dalton Trans.* **2003**, 2718–2727.

[20] L. Arnold, H. Norouzi-Arasi, M. Wagner, V. Enkelmann, K. Müllen, *Chem. Commun.* **2011**, *47*, 970–972.

[21] K. A. Connors, *Binding Constants*, Wiley, New York, **1987**.

[22] a) A. D. Becke, *Phys. Rev. A* **1988**, *38*, 3098–3100; b) C. Lee, W. Yang, R. G. Parr, *Phys. Rev. B* **1988**, *37*, 785–789; c) S. Grimme, J. Antony, S. Ehrlich, H. Krieg, *J. Chem. Phys.* **2010**, *132*, 154104; d) F. Weigend, R. Ahlrichs, *Phys. Chem. Chem. Phys.* **2005**, *7*, 3297–3305.

[23] a) P. Pulay, *Chem. Phys. Lett.* **1983**, *100*, 151–154; b) S. Sæbø, P. Pulay, *Chem. Phys. Lett.* **1985**, *113*, 13–18; c) H.-J. Werner, F. R. Manby, P. J. Knowles, *J. Chem Phys.* **2003**, *118*, 8149–8160; d) H.-J. Werner, M. Schütz, *J. Chem. Phys.* **2011**, *135*, 144166.

[24] a) T. H. Dunning Jr., *J. Chem. Phys.* **1989**, *90*, 1007–1023; b) D. E. Woon, T. H. Dunning Jr., *J. Chem. Phys.* **1993**, *98*, 1358–1371.

[25] C. Garau, D. Quiñonero, A. Frontera, P. Ballester, A. Costa, P. M. Deyà, *J. Phys. Chem. A* **2005**, *109*, 9341–9345.

[26] a) C. Garau, A. Frontera, D. Quiñonero, P. Ballester, A. Costa, P. M. Deyà, *Chem. Phys. Lett.* **2003**, *382*, 534–540; b) C. Garau, D. Quiñonero, A. Frontera, P. Ballester, A. Costa, P. M. Deyà, *New J. Chem.* **2003**, *27*, 211–214; c) C. Garau, A. Frontera, P. Ballester, D. Quiñonero, A. Costa, P. M. Deyà, *Eur. J. Org. Chem.* **2005**, 179–183; d) D. Quiñonero, C. Garau, A. Frontera, P. Ballester, A. Costa, P. M. Deyà, *J. Phys. Chem. A* **2005**, *109*, 4632–4637; e) A. Frontera, D. Quiñonero, C. Garau, A. Costa, P. Ballester, P. M. Deyà, *J. Phys. Chem. A* **2006**, *110*, 9307–9309; f) D. Quiñonero, A. Frontera, C. Garau, P. Ballester, A. Costa, P. M. Deyà, *ChemPhysChem* **2006**, *7*, 2487–2491; g) A. Frontera, D. Quiñonero, A. Costa, P. Ballester, P. M. Deyà, *New J. Chem.* **2007**, *31*, 556–560; h) C. Garau, D. Quiñonero, A. Frontera, D. Escudero, P. Ballester, A. Costa, P. M. Deyà, *Chem. Phys. Lett.* **2007**, *438*, 104–108; i) D. Quiñonero, A. Frontera, D. Escudero, P. Ballester, A. Costa, P. M. Deyà, *ChemPhysChem* **2007**, *8*, 1182–1187; j) D. Kim, P. Tarakeshwar, K. S. Kim, *J. Phys. Chem. A* **2004**, *108*, 1250–1258.

[27] A. Clements, M. Lewis, *J. Phys. Chem. A* **2006**, *110*, 12705–12710.

[28] a) J. Hernández-Trujillo, A. Vela, *J. Phys. Chem.* **1996**, *100*, 6524–6530; b) J. Hernández-Trujillo, M. Costas, A. Vela, *J. Chem. Soc. Faraday Trans.* **1993**, *89*, 2441–2443; c) J. R. Trudell, *Biophys. Chem.* **1998**, *73*, 7–11; d) R. J. Doerksen, A. J. Thakkar, *J. Phys. Chem. A* **1999**, *103*, 10009–10014; e) A. Alparone, *J. Fluorine Chem.* **2012**, *144*, 94–101.

[29] M. Giese, M. Albrecht, C. Bannwarth, G. Raabe, A. Valkonen, K. Rissanen, *Chem. Commun.* **2011**, *47*, 8542–8544.

[30] S. Grimme, *J. Chem. Phys.* **2003**, *118*, 9095–9102.

[31] a) J. G. Hill, J. A. Platts, H. J. Werner, *Phys. Chem. Chem. Phys.* **2006**, *8*, 4072–4078; b) S. Grimme, *Chem. Eur. J.* **2004**, *10*, 3423–3429; c) M. Piacenza, S. Grimme, *J. Am. Chem. Soc.* **2005**, *127*, 14841–14848; d) M. Piacenza, S. Grimme, *ChemPhysChem* **2005**, *6*, 1554–1558; e) T. Takatani, C. D. Sherrill, *Phys. Chem. Chem. Phys.* **2007**, *9*, 6106–6114; f) T. Van Mourik, A. K. Wilson, T. H. Dunning Jr., *Mol. Phys.* **1999**, *96*, 529–547.

[32] O. B. Berryman, V. S. Bryantsev, D. P. Stay, D. W. Johnson, B. P. Hay, *J. Am. Chem. Soc.* **2007**, *129*, 48–58.

[33] M. Schütz, G. Rauhut, H. J. Werner, *J. Phys. Chem. A* **1998**, *102*, 5997–6003.

[34] C. Garau, A. Frontera, D. Quiñonero, P. Ballester, A. Costa, P. M. Deyà, *Chem. Phys. Lett.* **2004**, *392*, 85–89.

[35] S. E. Wheeler, K. N. Houk, *J. Phys. Chem. A* **2010**, *114*, 8658–8664.

[36] a) M. Albrecht, M. Müller, O. Mergel, K. Rissanen, A. Valkonen, *Chem. Eur. J.* **2010**, *16*, 5062–5069; b) M. Müller, M. Albrecht, J. Sackmann, A. Hoffmann, F. Dierkes, A. Valkonen, K. Rissanen, *Dalton Trans.* **2010**, *39*, 11329–11334; c) V. S. Bryantsev, B. P. Hay, *J. Am. Chem. Soc.* **2005**, *127*, 8282–8283; d) B. P. Hay, T. K. Firman, B. A. Moyer, *J. Am. Chem. Soc.* **2005**, *127*, 1810–1819; e) O. B. Berryman, A. C. Sather, B. P. Hay, J. S. Meisner, D. W. Johnson, *J. Am. Chem. Soc.* **2008**, *130*, 10895–10897; f) L. Pedzisa, B. P. Hay, *J. Org. Chem.* **2009**, *74*, 2554–2560; g) B. P. Hay, *Chem. Soc. Rev.* **2010**, *39*, 3700–3708; h) M. Schnopp, S. Ernst, G. Haberhauer, *Eur. J. Org. Chem.* **2009**, 213–222; i) D. W. Yoon, D. E. Gross, V. M. Lynch, J. L. Sessler, B. P. Hay, C. H. Lee, *Angew. Chem.* **2008**, *120*, 5116–5120; *Angew. Chem. Int. Ed.* **2008**, *47*, 5038–5042.

[37] a) J. P. Foster, F. Weinhold, *J. Am. Chem. Soc.* **1980**, *102*, 7211–7218; b) A. E. Reed, F. Weinhold, *J. Chem. Phys.* **1983**, *78*, 4066–4073; c) A. E. Reed, F. Weinhold, *J. Chem. Phys.* **1985**, *83*, 1736–1740; d) A. E. Reed, R. B. Weinstock, F. Weinhold, *J. Chem. Phys.* **1985**, *83*, 735–746; e) A. E. Reed, L. A. Curtiss, F. Weinhold, *Chem. Rev.* **1988**, *88*, 899–926.

[38] V. S. Bryantsev, B. P. Hay, *Org. Lett.* **2005**, *7*, 5031–5034.

[39] G. Sheldrick, *Acta Crystallogr. Sect. A* **2008**, *64*, 112–122.
[40] X-RED, STOE & CIE, Darmstadt (Germany), **2002**.
[41] a) R. Ahlrichs, *Phys. Chem. Chem. Phys.* **2004**, *6*, 5119–5121; b) F. Neese, F. Wennmohs, A. Hansen, U. Becker, *Chem. Phys.* **2009**, *356*, 98–109; c) F. Neese, *J. Comput. Chem.* **2003**, *24*, 1740–1747.
[42] F. Neese, *Comput. Mol. Sci.* **2012**, *2*, 73–78.
[43] H.-J. Werner, P. J. Knowles, G. Knizia, F. R. Manby, M. Schütz, P. Celani, T. Korona, R. Lindh, A. Mitrushenkov, G. Rauhut, K. R. Shamasundar, T. B. Adler, R. D. Amos, A. Bernhardsson, A. Berning, D. L. Cooper, M. J. O. Deegan, A. J. Dobbyn, F. Eckert, E. Goll, C. Hampel, A. Hesselmann, G. Hetzer, T. Hrenar, G. Jansen, C. Köppl, Y. Liu, A. W. Lloyd, R. A. Mata, A. J. May, S. J. McNicholas, W. Meyer, M. E. Mura, A. Nicklass, D. P. O'Neill, P. Palmieri, D. Peng, K. Pflüger, R. Pitzer, M. Reiher, T. Shiozaki, H. Stoll, A. J. Stone, R. Tarroni, T. Thorsteinsson, M. Wang, http://www.molpro.net, **2012**.
[44] a) F. Weigend, *Phys. Chem. Chem. Phys.* **2002**, *4*, 4285–4291; b) F. Weigend, A. Köhn, C. Hättig, *J. Chem. Phys.* **2002**, *116*, 3175.
[45] J. Pipek, P. G. Mezey, *J. Chem. Phys.* **1989**, *90*, 4916–4926.
[46] R. A. Mata, H.-J. Werner, *Mol. Phys.* **2007**, *125*, 2753–2761.
[47] E. D. Glendening, J. K. Badenhoop, A. E. Reed, J. E. Carpenter, J. A. Bohmann, C. M. Morales, F. Weinhold, http://www.chem.wisc.edu/~nbo5, Theoretical Chemistry Institute, University of Wisconsin, Madison, WI, **2009**.

Received: July 4, 2013
Published online: November 6, 2013

